Morphological Variations in Polymer Blends Made in Electric Fields

Ganesh Venugopal,† Sonja Krause,* and Gary E. Wnek

Department of Chemistry and Polymer Science and Engineering Program, Rensselaer Polytechnic Institute, Troy, New York 12180-3590

Received June 18, 1992. Revised Manuscript Received September 10, 1992

The effects of electric fields on the morphologies of a number of binary multiphase polymer blend systems have been studied. The electric fields were applied while the blends were being solvent cast from single-phase solutions. Blends which were made up of polymers with different dielectric constants interacted with the electric fields to produce anisotropic morphologies. In all these systems polystyrene (PS), which was chosen to be the polymer with lower dielectric constant, formed the matrix phase. The minor phases were formed by poly(methyl methacrylate) (PMMA), poly(ethylene oxide) (PEO), poly(*o*-toluidine) (POT), or poly(vinyl acetate) (PVAc). PS–polybutadiene (PB), a blend of polymers with similar dielectric constants, showed no change in morphology when compared to the zero-field case. A whole range of compositions was studied for one PMMA–PS system and showed that anisotropic phases were formed only in systems in which PS formed the matrix. The zero-field morphologies of this system indicated that the critical point in the PS–PMMA–toluene phase diagram is at about 75% PMMA, in good agreement with the value calculated from Flory–Huggins theory. The PEO–PS system prepared from toluene showed a behavior similar to that made from cyclohexanone, although the columns in the blends prepared from toluene solutions appeared to be more stable against Rayleigh instability breakup.

Introduction

Multiphase polymer blends in which the minor phases are oriented in a desired direction should demonstrate unique electrical, optical, and mechanical properties. For example, if the minor phase is made up of conducting polymer, high electric conductivities or dielectric constants are expected in the direction of orientation. Or, a blend in which a polymer is dispersed and oriented in a matrix of another polymer is expected to have different mechanical properties parallel and perpendicular to the direction of orientation.

In a preliminary study[1] that was carried out earlier with poly(ethylene oxide) (PEO)–polystyrene (PS) blends, we reported that electric fields could be used to form minor phases with anisotropic structures. The electric fields were applied while the blends were being solvent cast from homogeneous solutions of two polymers in cyclohexanone. Phase separation during solvent removal and the interaction of the resultant phases with the applied electric fields produced oriented phases. After complete solvent removal, the orientation of these phases was preserved even after the electric field was removed. The morphologies of the blends were found to depend on the magnitude of the electric field and on the molecular weights of the PEO used. For example, low molecular weight PEO blends showed a pearl-chain morphology at 10 kV/cm. In this morphology the minor phases are organized like strings of pearls, each string being oriented in the direction of the electric field. Such structural organization has also been observed in colloidal dispersions which are known to form electrorheological fluids.[2] At the same field, in the higher molecular weight PEO blends, the minor phases deformed into columnar structures which were oriented in the electric field direction. Some of the columns in the blends appeared to be at a point of break-up due to the phenomenon called *Rayleigh instability*.[3]

The study of electric-field-induced deformation processes in multiphase systems is not new. While investigating the electric breakdown mechanisms in insulating oils, Garton and Krascuki[4] studied the effects of electric fields on water drops dispersed in these oils. They found that at high fields (~1 MV/cm) the water drops elongated in the direction of the field to form conduction pathways between the electrodes. Such a process will occur under two conditions: (1) the drop has to be deformable (nonrigid) and located in a nonrigid matrix; (2) the difference in the dielectric constants between the drop (κ_d) and the suspending phase (κ_m) has to be nonzero. As described by Garton and Krascuki,[4] the strength of the electric field required to bring about such a deformation depends on (1) the magnitude of the difference in dielectric constants, (2) the interfacial tension between the two phases, σ, and (3) the radius of the suspended phase. The electric field strength (E, V/cm) required to deform a spherical drop of radius r (cm) into a prolate ellipsoid of deformation ratio (ratio between the major semiaxis and the minor semiaxis of the ellipsoid) B could then be given by the equation[4]

$$E = 600\left(\frac{\pi\sigma}{\kappa_m r}\right)^{1/2}\left(\frac{\kappa_m}{\kappa_d - \kappa_m} - G\right)H \qquad (1)$$

where G and H are geometrical parameters that are functions of B, and σ is in dyn/cm. Equation 1 predicts that as the electric field is increased so is the deformation ratio of the phase. In the water-in-oil experiment, above a threshold field strength, an ellipsoidal water phase became unstable and ejected smaller water droplets from the ends until stability was restored at lower values of r, i.e., a maximum in deformation ratio was observed at a threshold value of E. This behavior, commonly referred to as *burst behavior*, is predicted by eq 1 if κ_d/κ_m is greater than 20 in the sense that the predicted deformation ratio *decreases* above the threshold value of E.

The pearl-chaining effect occurs because of a phenomena called *mutual dielectrophoresis*.[5] Dielectrophoresis is the

† Current address: AT&T Bell Laboratories, Murray Hill, NJ 07974.

(1) Venugopal, G.; Krause, S.; Wnek, G. E. *J. Polym. Sci., Polym. Lett.* **1989**, *27*, 497.
(2) Block, H., Kelly, J. P. *J. Phys. D.: Appl. Phys.* **1988**, *21*, 1661.
(3) (a) Rayleigh, J. W. S. *Proc. R. Soc. London* **1879**, *29*, 71. (b) Tomotika, S. *Proc. R. Soc. London, A* **1935**, *150*, 322.
(4) Garton, C. G.; Krascuki, Z. *Proc. R. Soc. London, A* **1964**, *280*, 221.
(5) Pohl, H. A. *Dielectrophoresis*; Cambridge University Press: Cambridge, 1978.

0897-4756/92/2804-1334$03.00/0

Table I. Molecular Weights and Dielectric Constants of Polymers

code	polymer	M_w ($\times 10^{-3}$)[e]	M_w/M_n[e]	κ[f]
PS220[a]	polystyrene	217	2.07	2.49–2.55
PEO10[a]	poly(ethylene oxide)	10.5	1.17	4.5
PEO100[a]	poly(ethylene oxide)	100[g]		4.5
PMMA16[b]	poly(methyl methacrylate)	15.9	1.61	3.6
PMMA38[b]	poly(methyl methacrylate)	38.7	1.87	3.6
PMMA88[a]	poly(methyl methacrylate)	88.2	1.98	3.6
PMMA120[c]	poly(methyl methacrylate)	122	1.98	3.6
PVAc[b]	poly(vinyl acetate)	100[g]		3.5
POT-B	poly(*o*-toluidine)	6.5	4.02	NA[h]
PB[d]	polybutadiene	250[g]		2.51

[a] Aldrich Chemical Co., Inc., Milwaukee, WI. [b] Scientific Polymer Products (SP²), Inc., Ontario, NY. [c] Du Pont de Nemours, Inc., Wilmington, DE. [d] Miles, Inc., Orange, TX. [e] Molecular weights and molecular weight distributions determined by gel permeation chromatography, unless otherwise specified. [f] Dielectric constant data from ref 11. [g] Data from supplier. [h] NA: not available.

translational motion of neutral matter in the presence of an inhomogeneous electric field. For multiphase systems in an electric field, if the dielectric constant of the dispersed phase differs from the dielectric constant of the matrix, an interfacial polarization mechanism distorts the applied field to produce a field inhomogeneity within the system. The region of highest field exists at the interface; therefore two dispersed particles are drawn toward each other.

Pohl[5] and Schwan et al.[6] have examined this process theoretically. By equating the ordering force produced by interfacial polarization with the randomizing force, Brownian motion, Pohl[5] derived the following expression (in MKS units) for the threshold field strength (E_p) required for observing pearl-chain formation:

$$E_p = \left|\frac{\kappa_d + 2\kappa_m}{\kappa_m - \kappa_d}\right|\left(\frac{kT}{2\pi\epsilon_0\kappa_m r^3}\right)^{1/2} \quad (2)$$

where T denotes the absolute temperature, k the Boltzman constant, and ϵ_0 the permittivity of free space. The larger the difference in the dielectric constants, the lower is E_p. In the event that $\kappa_m = \kappa_d$, E_p is infinity, because no interfacial polarization occurs. It can also be seen from eq 2 that E_p decreases with increase in particle size. This prediction has been qualitatively verified experimentally by Schwan et al.[6]

In this work we have extended the study of the effects of electric fields on binary blends to include a larger number of systems consisting of polymers with different dielectric constants, since, as predicted by the theory, the larger the difference in the dielectric constants the lower the electric fields required to observe morphology changes. The mixtures that were studied included poly(methyl methacrylate) (PMMA)–PS, PEO–PS, poly(*o*-toluidine) (POT)–PS, and poly(vinyl acetate) (PVAc)–PS. One blend of polymers with similar dielectric constants, polybutadiene (PB)–PS, was also studied for comparison. Most of the blends were prepared using toluene as the solvent. A range of PMMA–PS compositions was examined so that the effect of phase inversion could be studied. Furthermore, in the PEO–PS case, by making comparisons with results from our previous publication,[1] some conclusions about possible effects of solvent changes could be made.

Experimental Section

Materials. The molecular weight data of all the polymer samples studied in this work are listed in Table I. Molecular weights were determined by either gel permeation chromatography (GPC) or vapor-phase osmometry (VPO) as described below. In some cases, these data were provided by the supplier of the sample. GPC measurements were carried out in tetrahydrofuran on a Waters GPC instrument. A single linear column (Ultrastyragel, molecular weight range 2×10^3–4×10^6) was used, and the peaks were detected by a Waters R40 differential refractometer. Molecular weight calibration was done using PS standards for PS and POT-B samples, and PMMA standards for PMMA and PEO samples. Both calibration standards kits were purchased from Scientific Polymer Products.

Poly(*o*-toluidine) (POT) was synthesized following the procedure originally used by Willstatter et al.[7] for the synthesis of polyaniline. That is, *o*-toluidine was polymerized by chemical oxidation with ammonium persulfate. About 11 g of *o*-toluidine was dissolved in approximately 300 mL of 1 M hydrochloric acid. The solution was cooled in an ice bath to less than 5 °C, and a few milligrams of ferrous sulfate were added to it as a catalyst. An ammonium persulfate solution (100 mL of a 0.2 M solution) was added dropwise to the *o*-toluidine solution, and the final mixture left in a freezer for 2 h. The mixture was filtered and gave the conducting, salt form of poly(*o*-toluidine) (POT-S). The salt was washed with 1 M HCl solution until the filtrate became colorless, then refiltered, and dried. Half the amount of polymer was converted to the nonconducting base (POT-B) form by stirring with ammonium hydroxide at a pH of 9.2. A number average molecular weight (M_n) of 2×10^3 g/mol was measured for the POT-B sample in chloroform by vapor-pressure osmometry (VPO) on a Knauer Model 11 VPO unit (the value obtained by GPC in THF was 1.6×10^3 g/mol). Benzil (Aldrich, purified by sublimation at 70 °C) was used as a calibrant.

All polymer samples were used as received, without any further purification. Solvent casting was done from 4% solutions (i.e., 4 g of polymer/100 mL of solvent) in cyclohexanone (Fisher Scientific, purified by vacuum distillation) or toluene (Aldrich Chemical Co., HPLC grade). Approximately 0.2 mL of solution was used. About 30 min was required for complete solvent evaporation at room temperature.

Some solvent-cast PMMA–PS blends were stained with ruthenium tetroxide. One at a time, glass microscope slides coated with the blend films were placed in a 250-mL bottle which contained about 10 mL of a 0.5% (by weight) solution of ruthenium tetroxide in water (purchased from Polysciences, Inc.). Staining of each sample was carried out for about 2–3 h. Trent et al.[8] have reviewed the staining properties of ruthenium tetroxide for polymers.

Application of Electric Fields. Electric fields of up to 15 kV/cm could be applied using a Hewlett-Packard 6516A high-voltage dc power supply. A detailed description of the setup used for the application of the electric fields has been given elsewhere.[9] Two types of electrodes were used to apply electric fields to the samples. The first and most often used type was made by evaporating either aluminum or copper metal onto glass microscope slides.[9] This electrode design will be referred to as the type I electrode and unless otherwise specified was the design used for all the experiments. Metal evaporation was done using a tungsten basket in a CVC high-vacuum evaporator. Masks made out of 3M Scotch tape were used to coat the slides selectively. From the amount of metal used and the distance between the basket and the slide, the electrode thickness was estimated to be about 0.1 μm. The gap between the electrodes was usually about 2 mm. Occasionally, another type of electrode (which will be referred to as the type II electrode) was used. This was prepared by taping two strips of adhesive-backed 3M Scotch brand copper or aluminum tape (Ernest F. Fullam, Inc.) 2 mm from each other onto glass microscope slides. The type II electrodes were similar in design to the type I electrodes,[9] except thicker (approximately 1 mm).

Optical microscopy was done on a Leitz Laborlux 12 Pol S microscope. Since the blends were solvent cast on microscope

(6) Schwan, H. P.; Sher, L. D. *J. Electrochem. Soc.* **1969**, *22c*, 116.

(7) Willstatter, R.; Dorogi, S. *Chem. Ber.*, **1909**, *42*, 2143.

(8) Trent, J. S.; Scheinbeim, J. I.; Couchman, P. R. *J. Polym. Sci., Polym. Lett. Ed.*, **1981**, *19*, 315.

(9) Venugopal, G.; Krause, S. *Macromolecules*, in press.

slides, they could be studied without further sample preparation. Morphologies were recorded using either a 35-mm SLR camera or a Polaroid Instant camera. The eyepiece lens had a magnification of 10×. The magnification of the objective was either 10×, 25×, or 40× and depended on the sizes of the structures being studied.

Results and Discussion

Blends Containing More Than 70% PS. The electric-field-induced morphology changes observed in PEO-PS blends made from toluene parallel those that were seen for the same blends made from cyclohexanone.[1] The change of casting solvent, from cyclohexanone[1] to toluene, was made because toluene solutions underwent much less electric-field-induced solution motion when compared to cyclohexanone solutions.[10] This may be because toluene has a lower dielectric constant than cyclohexanone.

The morphologies of a PEO10-PS220 blend and PEO100-PS220 blend made from toluene under zero field conditions are shown in Figure 1, parts a and c, respectively. Both systems exhibit spherical phases of PEO uniformly dispersed in a PS matrix, with the PEO phases in the PEO100-PS220 blend being slightly larger than those in the PEO10-PS220 blend. Figure 1b,d shows the morphologies of the PEO10-PS220 and PEO100-PS220 blends made by solvent casting from a toluene solution in a 12.5 kV/cm electric field. While the blend containing the lower molecular weight PEO shows a pearl-chained structure, the PEO100-PS220 blend demonstrates columnar structures. In both cases, the structures are oriented in the direction of the electric field. In general, the sizes of the phases in blends cast in an electric field are larger than those cast outside the electric field. This increase is a result of a field induced *coalescence* process,[9] i.e., two fluid particles drawn toward each other either due to electric-field-induced dielectrophoresis or due to field-induced fluid motion,[10] fuse to form one particle which is larger in size.

The columnar structures seen in Figure 1d are a result of electric-field-induced phase deformation, a phenomenon similar to the one observed by Garton and Krasucki[4] in water in oil dispersions. The fact that the columnar structures are only visible in the high molecular weight PEO blend is most probably because this blend forms large phases that are easily deformed by the electric field (see eq 1). The columnar structures observed in the Figure 1d appeared more stable to Rayleigh instability breakup[3] than those seen in the same blend made from cyclohexanone.[1] It is difficult at this stage of our studies to isolate the exact reason for this increased stability since, by changing the solvent, we have changed the dielectric constants and the viscosities of the phases as well as the interfacial tensions between the phases. The factors governing Rayleigh instability are discussed further in the following section.

Columnar phases were also observed in the PMMA38-PS220 system. Figure 2 shows the morphology of the 10% PMMA38-PS220 blends made in (a) a 0 kV/cm electric field and (b) a 10 kV/cm electric field, respectively. Pearl-chaining could be obtained in the PPMA38-PS220 system only if the sizes of the minor phases were kept small; this could be done using the type II electrodes. The reason for the formation of smaller phases under these conditions is not clear, although one factor may be significant, namely, the more homogeneous electric fields that result from the use of thicker electrodes.[10] Less solution motion was observed when type II electrodes were used so that droplets of the dispersed phase did not collide as frequently as when type I electrodes were used, thereby reducing coalescence.

An example of the blends made using the type II electrodes outside and inside the electric field are shown in Figure 3, parts a and b, respectively. Note that pearl chains were obtained using the type II electrodes while columns were obtained using type I electrodes (see Figure 2b). It is therefore necessary to emphasize that the type of electrode used affected the type of morphology produced. Electrode designs which produced inhomogeneous fields (for example, the type I electrodes) apparently encouraged migration and aggregation of dispersed phases. Fusion of these aggregated phases leads to larger sized phases which have a tendency to deform more easily.

Anisotropic morphologies were observed with all but one of the polymer blends that contained more than 70% PS. The exception, the polybutadiene (PB)–PS blend solvent cast from toluene, showed no change in morphology due to the application of an electric field. This result is not surprising since the dielectric constant difference between the two polymers is very small[11] (2.51 for PB and between 2.49 and 2.55 for PS). The difference is further reduced because a large amount of toluene is present in both phases during solvent casting. The last column in Table I lists the dielectric constants for all the polymers used in this work.

Figure 4 shows the morphology of a 10% PVAc-PS220 system made (a) without a field and (b) with a 10 kV/cm field. While the zero-field morphology shows no peculiarities when compared to zero-field morphologies of other blends, the field-treated blend differs from other blends in that it shows deformed phase morphologies, ellipsoids and columns, and pearl-chain-like structures in the same sample.

Figure 5a shows the zero-field morphology of a POT-B-PS220 mixture cast from cyclohexanone. The weight ratio of the two polymers was 10:90; however, not all of the POT-B was dissolved. Figure 5b shows the morphology of the same blend made in a 7.5 kV/cm electric field. Short fiberlike structures of POT-B oriented in the direction of the field are seen. When the same experiment was done after filtering the polymer–polymer–solvent mixture through a 0.45-μm Teflon membrane, very few, if any, fibrillar structures were observed. This result suggests that the fibrous structures are not formed during phase separation, but rather by the deformation of cyclohexanone swollen POT-B particles that already exist in the mixture.

On the Stability of Columnar Structures. The pearl-chains seen in the 10% PVAc–PS220 sample, Figure 4b, are probably not formed by mutual dielectrophoresis, but rather occur because of an inherent instability of fluid cylinders. This instability is often referred to as the Rayleigh instability since it was first observed in fluid cylinders under flow by Lord Rayleigh.[3a] Due to this instability, cylindrical liquid phases in a fluid matrix can exhibit a breakup phenomenon whereby the cylinder is transformed into a number of smaller sized spheres. Unlike phase fusion, breakup results in an increase in interfacial area. Tomotika[3b] was the first person to study theoretically the instabilities of liquid cylinders in a liquid

(10) The type I electrodes are approximately 0.1 μm thick. When the solution is placed between the electrodes, a part of it flows over the electrodes. The electric field experienced by the solution is therefore quite inhomogeneous. This inhomogeneity causes a rippling motion which is also a consequence of dielectrophoresis.

(11) (a) *Polymer Handbook*, 3rd ed.; Brandrup, J., Immergut, E. H., Eds.; John Wiley and Sons: New York, 1989. (b) Blythe, A. R. *Electrical Properties of Polymers*; Cambridge University Press: Cambridge, 1979.

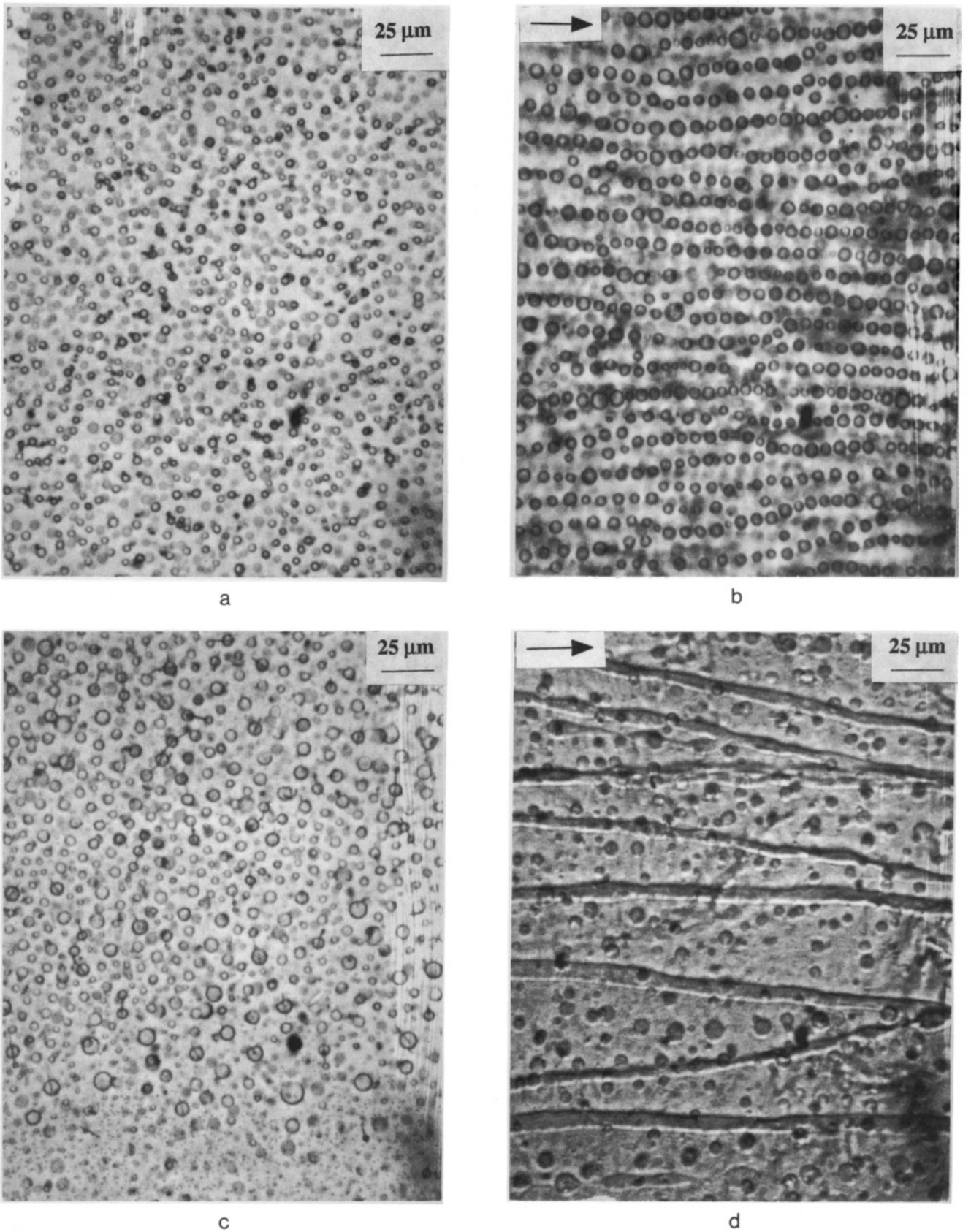

Figure 1. Morphologies of a PEO–PS220 blends solvent cast from toluene, as seen through an optical microscope: (a) 10% PEO10–PS220 cast under zero-field conditions, (b) 10% PEO10–PS220 cast in a 12.5 kV/cm electric field, (c) 10% PEO100–PS220 cast under zero-field conditions, and (d) 10% PEO100–PS220 cast in a 12.5 kV/cm electric field. The arrows indicate the direction of the electric field.

matrix. At first the cylinder (radius r_c) undergoes a sinusoidal distortion of wavelength λ. Distortions with a wavelength larger than the original circumference of the cylinder grow because the total interfacial area decreases with increase in amplitude. The growth rate (rate of growth of the amplitude of a sinusoidal distortion with time), q, is given by

$$q = \sigma\Omega(\lambda,P)/2\eta_m r_c \quad (3)$$

where $P = \eta_d/\eta_m$ and $\Omega(\lambda,P)$ is a function of λ and P that

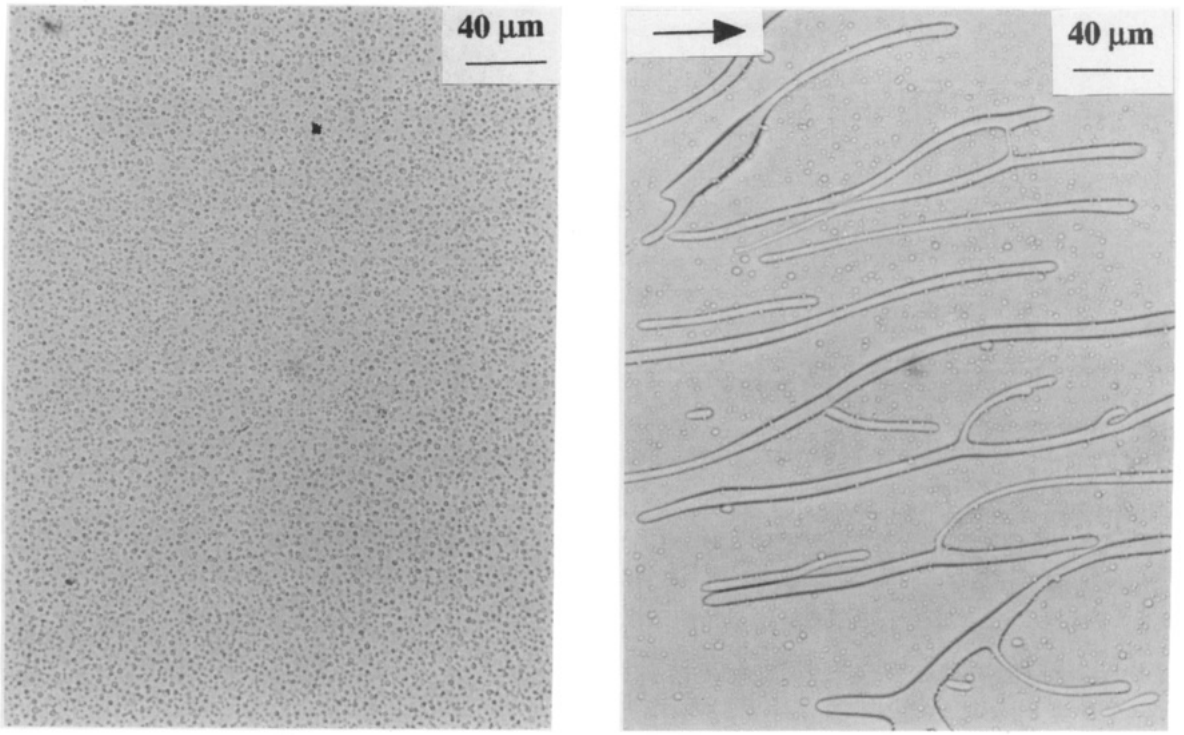

Figure 2. Optical micrographs showing the morphologies of a 10% PMMA38–PS220 blend cast from toluene: (a) sample cast in the absence of an electric field; (b) sample cast in a 10 kV/cm electric field. Arrow indicates the direction of the field.

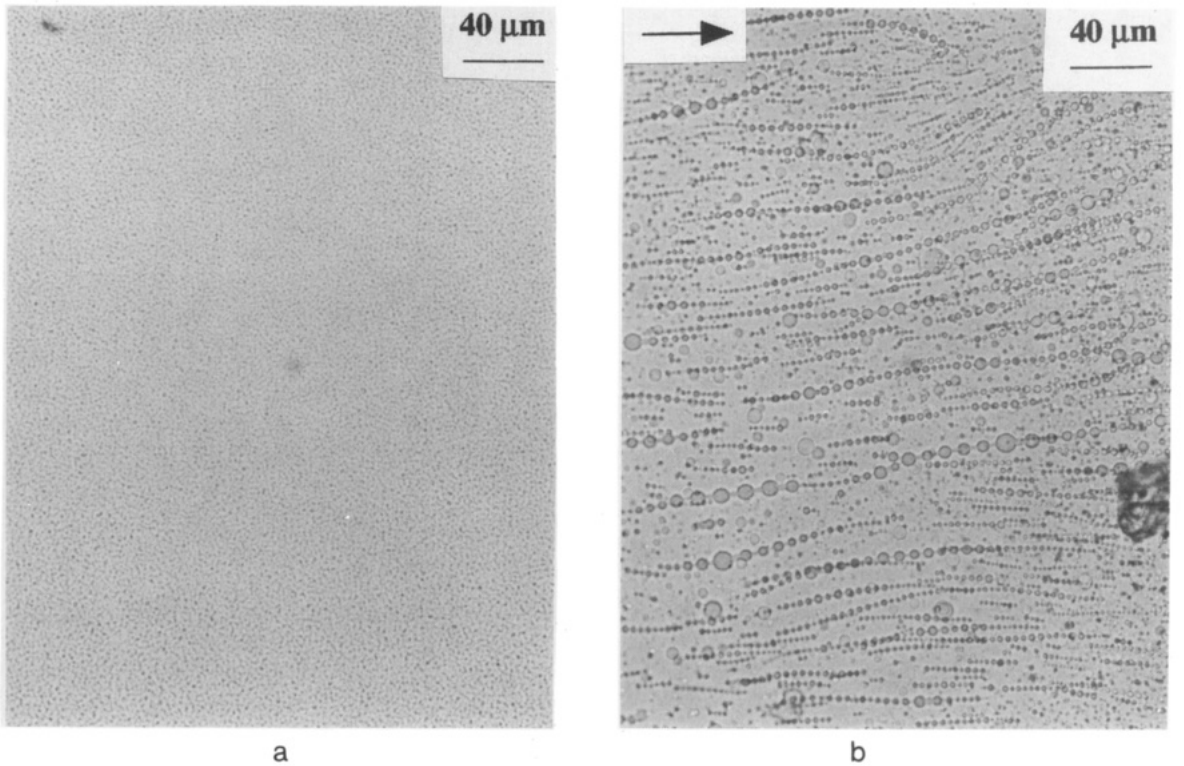

Figure 3. Optical micrographs showing the morphologies of a 10% PMMA38–PS220 blend cast from toluene using the type II electrode: (a) sample cast in the absence of an electric field and (b) sample cast in a 10 kV/cm electric field. Arrow indicates the direction of the field.

has been tabulated by Tomotika.[3b] The symbol η stands for viscosity, the subscripts d and m refer to drop and matrix, respectively.

In our earlier publication[1] we noted that PEO100–PS220 blends from cyclohexanone, in 10 kV/cm electric fields, displayed morphologies that resembled the structures seen here in the PVAc-PS blends, i.e. columnar structures which were partly pearl-chained. To explain these coexisting structures, two mechanisms were proposed: (1) formation of pearl chains followed by simultaneous deformation and fusion of the "pearls" in a single chain to form columns; (2) deformation of phases to columns, followed by Rayleigh instability breakup to form a string of smaller phases. Although no direct experimental evidence is available to

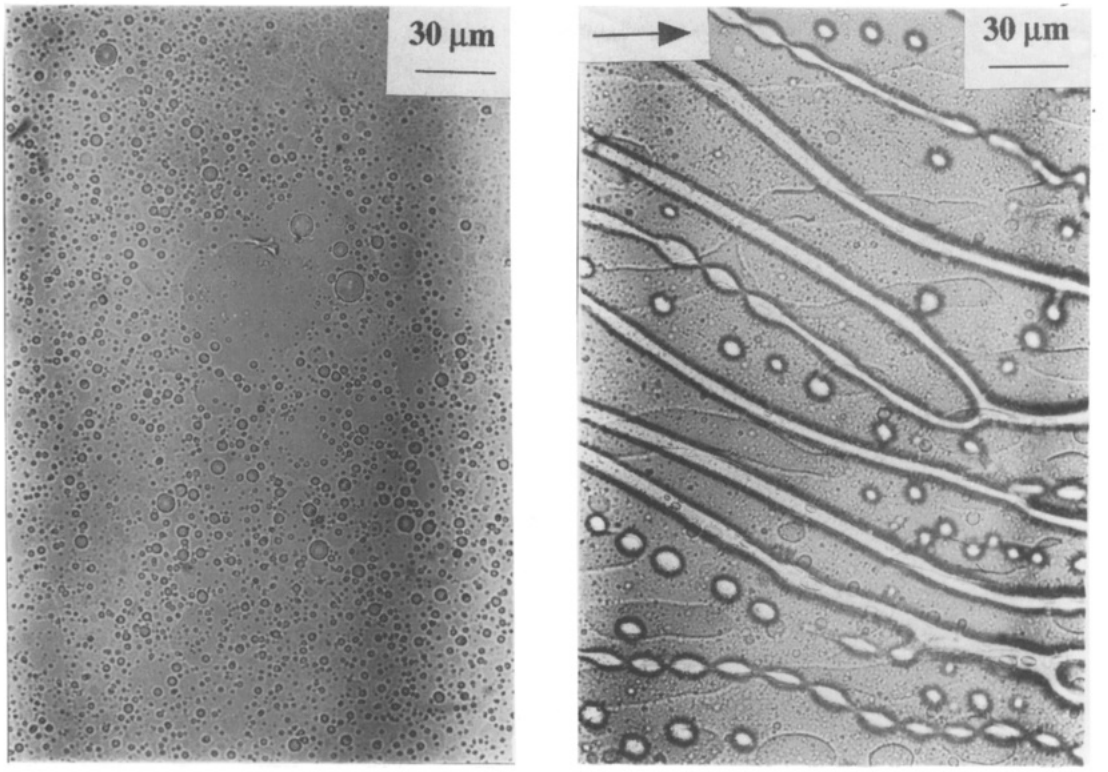

Figure 4. Morphologies of a 10% PVAc–PS220 blend cast from toluene in a (a) 0 kV/cm and (b) 10 kV/cm electric field, as seen through an optical microscope. Arrow indicates the direction of the electric field.

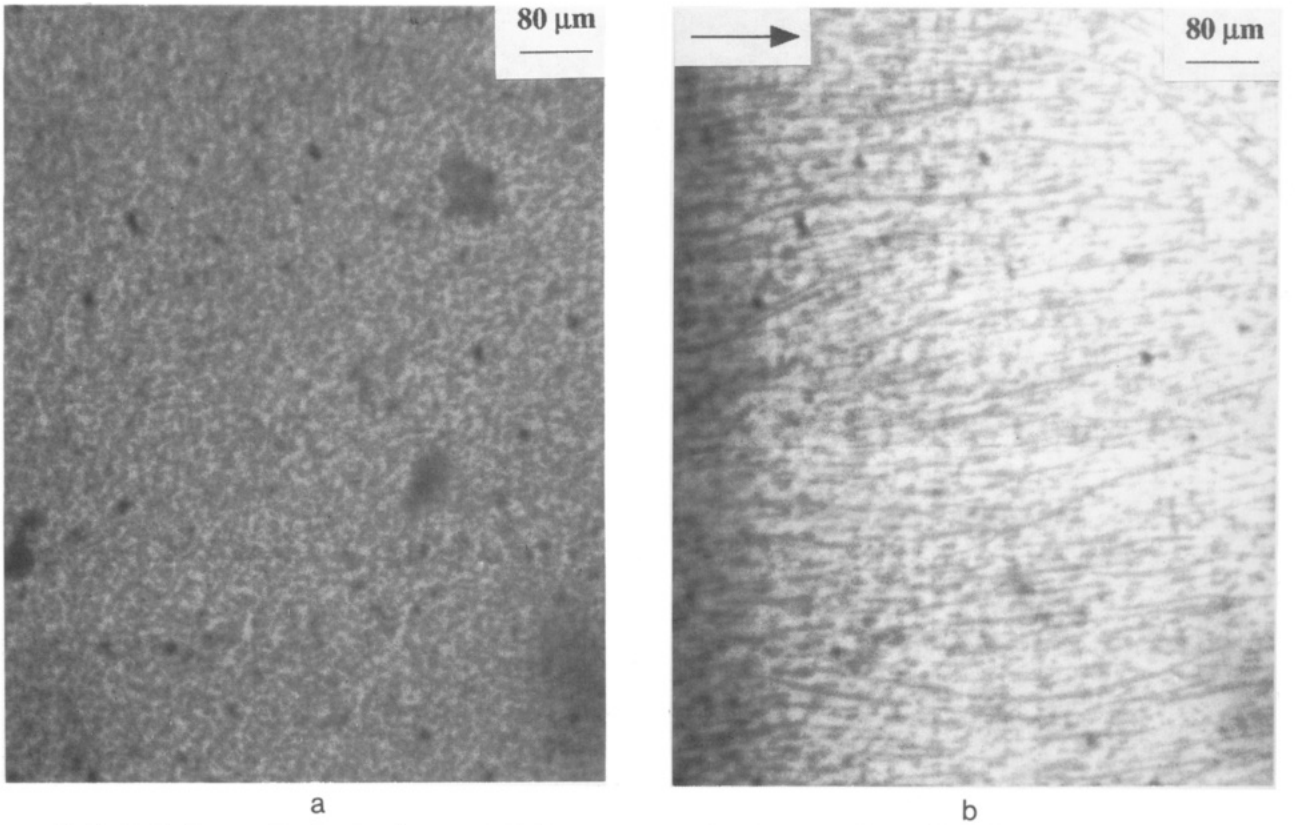

Figure 5. Optical micrographs showing the morphologies of an approximately 10% POTB–PS220 blend cast from cyclohexanone in a (a) 0 kV/cm electric field and (b) in a 7.5 kV/cm electric field. The arrow indictes the electric field direction.

favor either mechanism unambiguously, it is most likely that the second mechanism is the one favored in the PEO100–PS220 and PVAc–PS220 systems. This conclusion is based on the observation that the shapes of the "pearls" in the pearl-chains in Figure 4b do not resemble those of deformed droplets but rather are characteristic of drops formed by breakup due to Rayleigh instability.[12]

(12) Elemans, P. H. M.; Janssen, J. M. H.; Meijer, H. E. H. *J. Rheol.* **1991**, *34*, 1311.

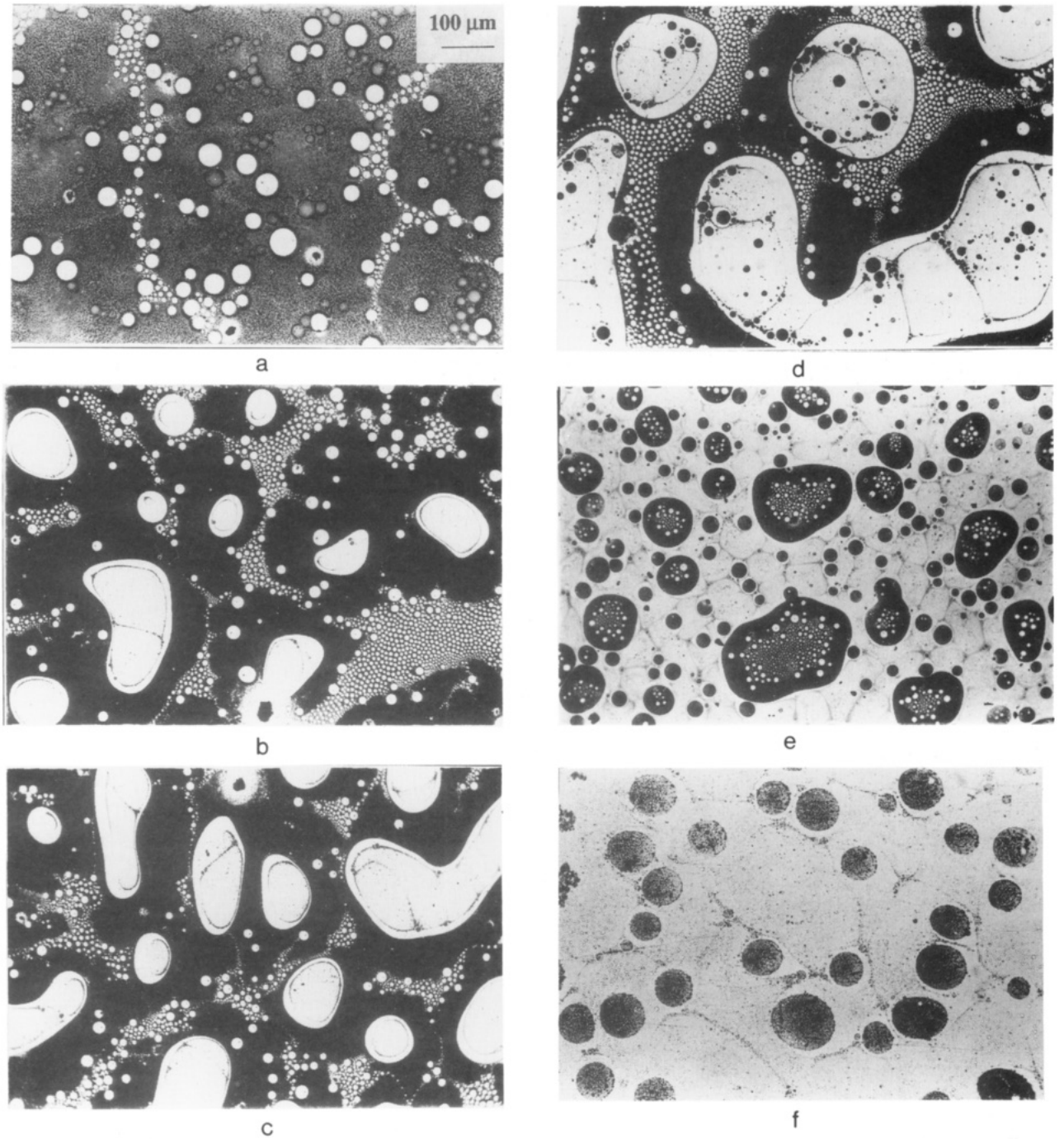

Figure 6. Zero-field morphologies of PPMA38–PS220 blends cast from toluene (various compositions). Ruthenium tetroxide was used to stain the PS-rich phases. The PMMA weight percents are (a) 40, (b) 50 (c) 60, (d) 70, (e) 80, and (f) 90. The scale shown in (a) also applies to the other micrographs is this figure.

We have also visually observed the Rayleigh instability process occurring in electric-field-deformed PMMA38-rich columns (in phase-separated PMMA38–PS220–toluene systems) after turning off the electric field before all the solvent had evaporated.[9]

Pearl-chain-like structures resulting from the breakup of columns may be seen in the final (solvent-free) morphologies of the blends only if the columnar morphology persists until the late stages of solvent casting, i.e., at low solvent concentrations. During this stage the viscosity of the system is high enough to prevent the electric-field-induced fluid motion from scattering the resulting spherical phases. The interfacial tension between the two phases is also expected to increase during solvent evaporation. Such an increase has been reported before for demixed polymer–polymer–solvent systems.[13] In some cases, for example for PVAc–PS case, such an increasing interfacial tension probably becomes a driving force for Rayleigh instability (see eq 3).

The columns formed by the PPMA–PS blends showed no Rayleigh instability; there is no indication of unstable columns in the morphology shown in Figure 2b. This is probably because the relatively high glass transition temperature (~105 °C) of the PMMA results in freezing of the columns before they can break up. PVAc, on the other hand, has a relatively low glass transition temperature (~30 °C)[11] and is thus relatively fluid even at lower solvent concentrations. This difference in variation of T_g with solvent concentration and also the variable evaporation

(13) Langhammer, G.; Nestler, L. *Makromol. Chem.* **1965**, *88*, 179.

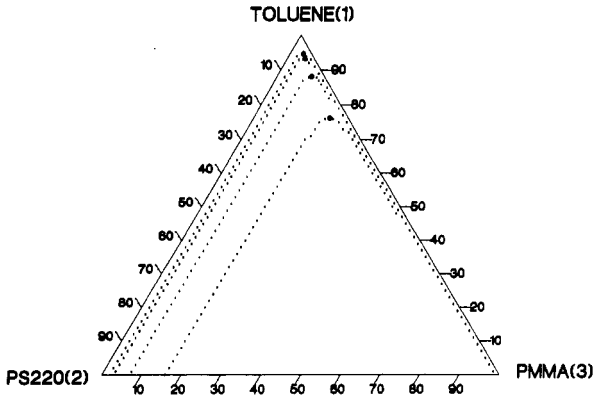

Figure 7. Calculated spinodal curves and critical points for PMMA(3)–PS220(2)–toluene(1) systems. Going from the inside of the phase diagram to the outside, the curves represent systems with PMMA molecular weights: 17×10^3, 38×10^3, 88×10^3, and 120×10^3. The interaction parameters used for the calculations are $\chi_{12} = 0.35$, $\chi_{13} = 0.40$, and $\chi_{23} = 0.02$.

rates from system to system influence the final morphology of the blends.

Poly(methyl methacrylate)–Polystyrene Blends with Less Than 70% PS. *Zero-Field Morphologies.* The final zero-field morphologies of PMMA38–PS220 blends of various compositions are shown in Figure 6. The dark regions in the micrographs are the RuO_4 stained polystyrene-rich phases; PMMA is not stained by RuO_4 and hence appears white. Blends with 40–70% PMMA show the presence of a PS matrix with PMMA dispersions. With increase in PMMA concentration the sizes of the dispersions get bigger. The morphologies of the blends which had 20 and 30% PMMA (not shown) showed similar dispersed PMMA phase behavior, although the PMMA phase sizes got smaller with decreasing PMMA concentration (the 10% PMMA case is shown in Figure 2a). The 80% and the 90% PMMA blends show a PMMA matrix with PS dispersions indicating that the phase inversion composition for this system, under the casting conditions used, is between 70% and 80% PMMA. In fact, in the 75% PMMA38–PS220 blend (not shown) no definite matrix could be observed. Hence we shall take this composition to be the phase inversion composition of the system. The appearance of PS phases within each PMMA inclusion in Figure 6d and that of the PMMA phases within each PS inclusion in Figure 6e is perhaps because both these blends are close to the phase inversion composition.

A wide range of phases sizes was observed for the 40% PMMA38–PS220 blend. This distribution of phase sizes may be explained by looking at Figure 7, which shows the calculated spinodal curves for PMMA–PS220–toluene systems for PMMA of four different molecular weights. These curves and their corresponding critical points were calculated as explained in an earlier paper[9] using Flory–Huggins theory.[14,15] The interaction parameters used for these calculations were $\chi_{12} = 0.35$, $\chi_{13} = 0.40$, and $\chi_{23} = 0.02$, where 1, 2, and 3 stand for toluene, PS, and PMMA, respectively. These interaction parameters were chosen because the spinodal curve calculated for one of them, the PMMA38–PS220–toluene system, lay within the binodal points (not shown here) that were obtained experimentally[9] for the same system. Judging by the large gap outside the spinodal in the low PMMA composition region of the PMMA38 case, one may predict that for blends with low

Table II. Comparison of Phase Inversion Compositions and Critical Point Compositions of Polymers in PMMA–PS–Toluene Systems

	vol fraction of PMMA in polymer portion of mixture	
system	at phase inversion (from morphology studies)	at the critical point (calculated)
PMMA17–PS220–toluene	0.80–0.90	0.79
PMMA38–PS220–toluene	~0.75	0.75
PMMA88–PS220–toluene	~0.70	0.71
PMMA120–PS220–toluene	0.60–0.70	0.60

PMMA compositions, the predominant phase separation mechanism is probably nucleation and growth, a mechanism which produces a heterogeneous distribution of phase sizes. Inoue et al.[16] have reached a similar conclusion for another PMMA ($M_w = 11 \times 10^4$ g/mol)–PS ($M_w = 22.4 \times 10^4$ g/mol)–toluene mixture using small-angle light-scattering experiments.

Of particular interest is the phase inversion composition for the system, observed at close to 75% for PMMA38–PS220 (see Figure 6). With increase in molecular weight of the PMMA, this phase inversion composition shifted to lower PMMA compositions. The approximate PMMA volume fractions of the PMMA/PS portion of the mixtures at phase inversion are shown in Table II. The PMMA volume fractions of the PMMA/PS portion of the mixtures at the critical points (from Figure 7) are also listed in Table II. These two sets of numbers are in qualitative agreement with each other, leading us to conclude that phase inversion is achieved upon crossing the critical point. This observation has been reported for two component polymer–solvent systems[17] and is of great importance in the field of membrane science.[18]

Electric-Field-Treated Morphologies. Figure 8 shows the final morphologies of the PMMA38-PS220 system (various compositions) when they were solvent cast from toluene in a 10 kV/cm electric field. The 40% PMMA blend, shown first (Figure 8a), exhibits a columnar morphology similar to the one shown by the 10% PEO100–PS220 and the 10% PMMA38–PS220 blends that were cast from toluene (Figures 1d and 2b). This 40% blend was the only one among the field-treated blends that was stained and indicates that the columns are composed of PMMA. Similar columnar morphologies are also shown by the 50% PMMA (Figure 8b) and the 60% PMMA (Figure 8c) blends. In all these blends only the large PMMA phases form columns, the smaller ones are seen to be ellipsoidal in shape. That the columns were formed by deformation and not by fusion of the pearls within the pearl chains was confirmed by monitoring the morphology evolution of a 20% PMMA38–PS220 with an optical microscope during solvent casting from toluene in an electric field.[9] These experiments showed that, as predicted by eq 1, increase in the electric field strength led to an increase in the deformation ratio of the PMMA-rich minor phases. Furthermore, as expected, since the κ_d/κ_m ratio in these systems is less than 2, no burst behavior was exhibited.

In the 70% PMMA38–PS220 (Figure 8d) and the 80% PMMA38–PS220 (Figure 8e) blend the number of deformed phases is greatly reduced as are the sizes of these phases. This happens because a majority of the PMMA

(14) Flory, P. J. *Principles of Polymer Chemistry*; Cornell University Press: Ithaca, NY, 1956.
(15) Tompa, H. *Polymer Solutions*; Butterworth: London, UK, 1956.
(16) Inoue, T.; Ougizawa, T.; Yasuda, O.; Miyasaka, K. *Macromolecules*, **1985**, *18*, 57.
(17) Kamide, K.; Manabe, S-I. In *Materials Science of Synthetic Membranes*; Lloyd, D. R., Ed.; American Chemical Society: Washington, DC, 1985.
(18) *Synthetic Membranes: Science, Engineering and Applications*; Bungay, P. M., Lonsdale, H. K., de Pinho, M. N., Eds.; D. Reidel: Dordrecht, Holland, 1986.

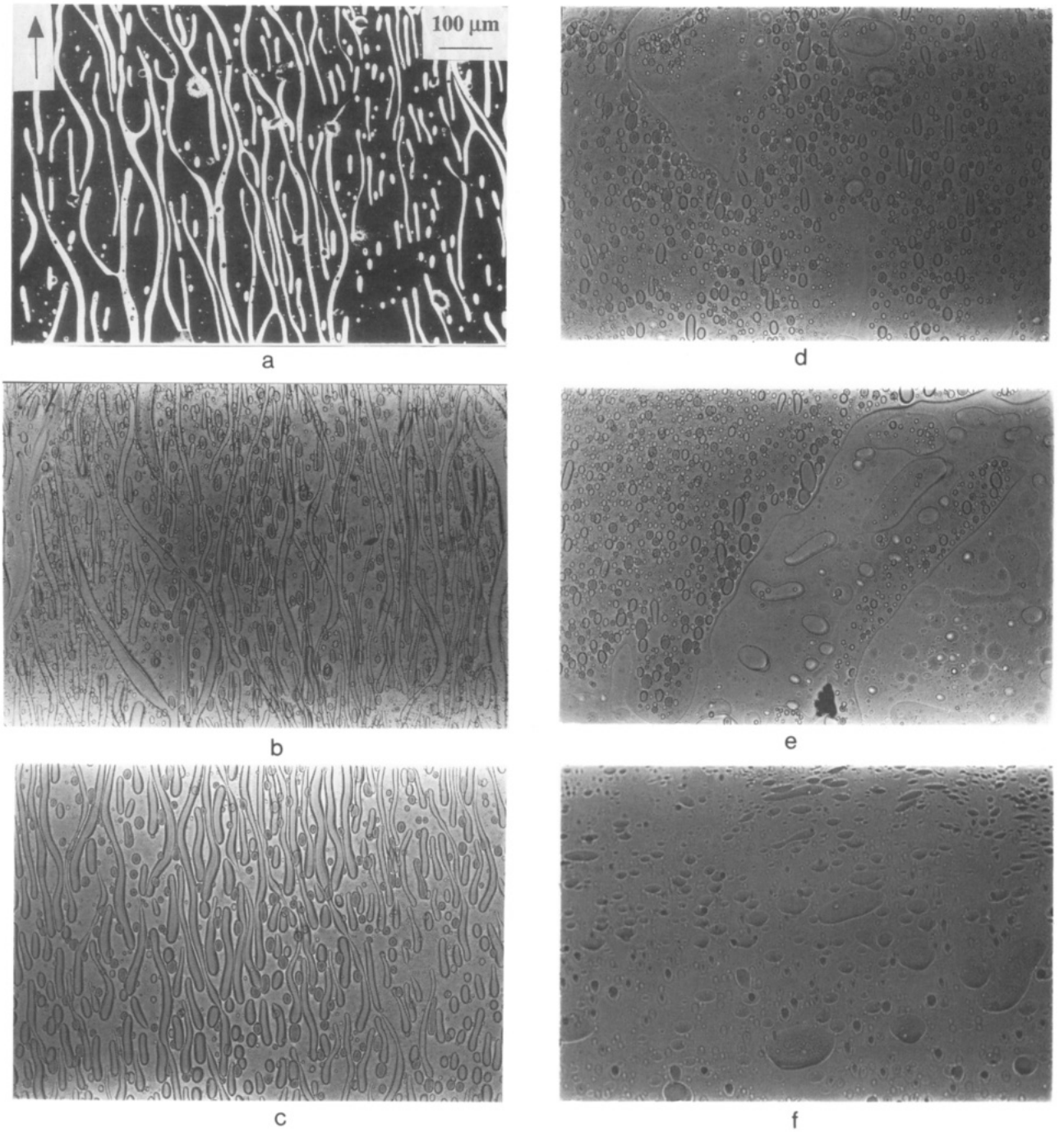

Figure 8. Optical micrographs growing the morphologies of PMMA38–PS220 blends (various compositions) cast from toluene in a 10 kV/cm electric field. The PMMA weight percents in the micrographs are (a) 40, (b) 50 (c) 60, (d) 70, (e) 80, and (f) 90. The 40% PMMA38 blend was stained with ruthenium tetroxide. The arrow in micrograph (a) indicates the direction of the electric field for all the samples. The scale shown on (a) also applies to the other micrographs in this figure.

now exists in separate regions where the PMMA itself forms the matrix. This was confirmed by staining the blends. For example, two optical micrographs, (a) unstained and (b) stained, of the same area of an 80% PMMA38–PS220 blend sample made from toluene in a 10 kV/cm field area shown in Figure 9, the PS phases in Figure 9b are stained with ruthenium tetroxide and hence appear black. The region where PS forms the matrix shows deformed minor phases while the other does not. The 90% (Figure 8f) blend shows a dispersed phase morphology with no significant deformation in the direction of the electric field (the phases that appear deformed perpendicular to the direction of the field were also observed, on occasion, in the same blends made outside the field).

From the micrographs in Figures 8 and 9, it is possible conclude that the phases that are deformed in the field direction appear only in the regions where PS forms the matrix. The major change in the system upon going from a PS matrix to a PMMA matrix is that in the latter the dielectric constant of the matrix, κ_m, is greater than that of the dispersed phase, κ_d. The theory of Garton and Krasucki[4] predicts that systems with $\kappa_m > \kappa_d$ should show droplet deformation just like systems with $\kappa_d > \kappa_m$.[19] The absence of deformed phases when PMMA forms the ma-

(19) Garton and Krasucki have shown in ref 4 that the extent of deformation of a drop in the electric field direction is a function of $(\kappa_m - \kappa_d)^2$. Hence, according to their theory, the drop will elongate in the field direction regardless of the sign of $(\kappa_m - \kappa_d)$.

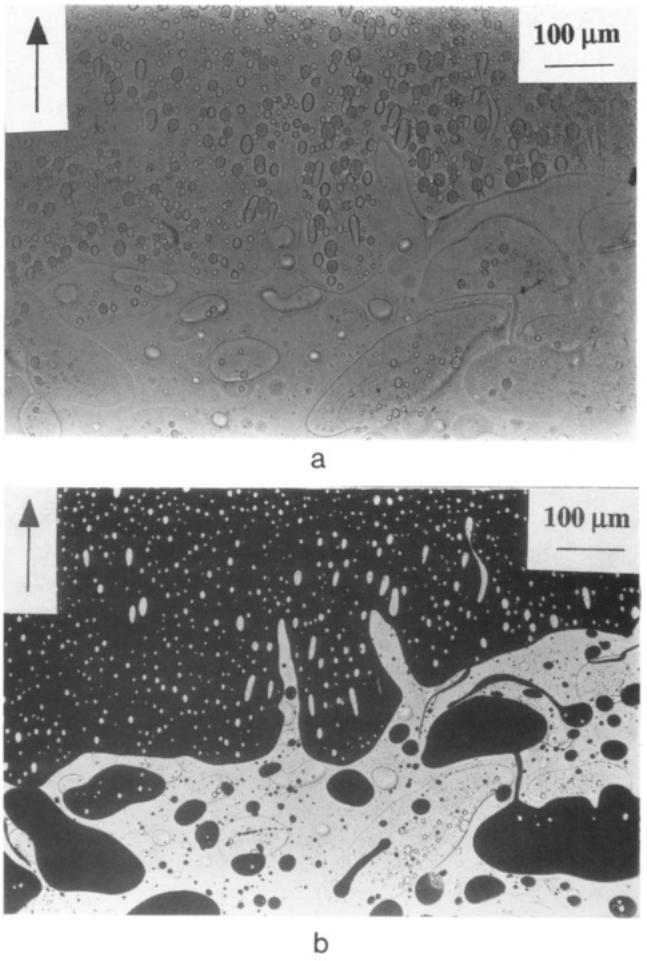

Figure 9. Optical photomicrographs of the morphologies of (a) unstained and (b) ruthenium tetroxide stained (same region as (a)), 80% PMMA38–PS220 blend cast from toluene in a 10 kV/cm electric field. The arrows indicate the electric field direction.

trix is an unexpected one and may be the result of the higher molecular weight of the PS sample used which leads to higher viscosities of the PS-rich phases. Alternatively, small quantities of impurities in our samples could make one or both phases conducting. In such a case the deformation characteristics of the drop phase depends not only on the ratio (D) of the dielectric constant of the drop to that of the matrix but also on the ratio (R) of the electrical resistivity of the drop to that of the matrix.[20] At $RD = 1$, the two phases are electrically indistinguishable and no deformation occurs. For a system with $RD < 1$ the drop deforms into a prolate ellipsoid, while for a system with $RD > 1$ the drop deforms into an oblate ellipsoid. Furthermore, as shown by Torza et al.,[20] the product RD also affects the frequency dependence of the deformation process.

(20) Torza, S.; Cox, R. G.; Mason, S. G. *Proc. R. Soc. London, A* **1971**, *269*, 295.

Conclusions

A number of phase separated binary blends of polar polymers and polystyrene were made by solvent casting in an electric field. In most of the cases the polystyrene formed the matrix phase. The electric field induced a number of modifications in the morphologies of these blends. These modifications depended on the nature of the polar polymer, their molecular weight, and composition with respect to polystyrene and also on the type of electrodes used.

(a) In blends which had relatively small phases (<10 μm in diameter), for example the PEO10–PS220 system, these phases could be oriented as pearl-chains in the direction of the electric field.

(b) In blends with larger phases, for example, PMMA38–PS220, PVAc–PS220, and PEO100–PS220, phase deformation in the direction of the electric field led to the formation of oriented ellipsoidal and columnar phases. The columns formed by PMMA appeared to be more stable to Rayleigh instability break up than those formed by the PVAc, probably because of the higher T_g of the PMMA.

In blends of PMMA38-PS220 from toluene (a) The phase inversion composition, which was estimated by studying the zero-field morphologies of the blends as a function of the percentage of PMMA38, gave a rough approximation of the critical point of the PPMA38–PS220-toluene system. This value was in reasonable agreement with a theoretical critical point value calculated for the same system using Flory–Huggins theory. (b) Electric-field-induced deformation of phases were observed only when PMMA formed the included phase, i.e., when PS formed the matrix phase. This change in behavior upon phase inversion is contrary to the theory of Garton and Krasucki[4] and may occur because the molecular weight of the PS sample was much higher than that of the PMMA sample.

Acknowledgment. Financial support for the project on which this paper is based was provided by the National Science Foundation under Grant DMR-9001054 and by DARPA in the form of a grant monitored by the Office of Naval Research.

Registry No. PS, 9003-53-6; PEO, 25322-68-3; PMMA, 9011-14-7; PVA, 9003-20-7; POT-B, 97917-08-3; PB, 9003-17-2; toluene, 108-88-3.